Supplementary information

Defect-rich molybdenum dioxide cluster coupled hierarchical carbon toward advanced Na-S batteries

Haonan Wanga+, Guangming Caoa+, Junquan Chenga, Bin Chena, Xin Xiaa, Youcun Baia*, Zhichao Yea, Baoxue Wanga, Feng Liua*, Heng Zhanga*

[a]Institute for Materials Science and Devices, School of Materials Science and Engineering, Suzhou University of Science and Technology, Suzhou 215009, P.R. China

+ Equal contributors

*Corresponding author: Youcun Bai, Feng Liu, Heng Zhang

E-mail address: ycbai@usts.edu.cn (Youcun Bai); feng.liu@usts.edu.cn (Feng Liu); zhangheng@usts.edu.cn (Heng Zhang)

Experimental:

All the chemical substances involved in this article are analytical grade components and have not undergone any purification. Ammonium molybdate ($(NH_4)_6Mo_7O_{24}\cdot 4H_2O$) and dopamine hydrochloride were purchased from Aladdin (China). The other reagents were purchased from Tansoole (China).

Synthesis of MoO_3 nanorods

One-dimensional MoO_3 nanorods were synthesized via a hydrothermal method. Typically, $NH_4)_6Mo_7O_{24}\cdot 4H_2O$, 710 mg) was dissolved in 20 mL of an aqueous HNO_3 solution (HNO_3: H_2O volume ratio = 1: 5). The resulting solution was transferred into a Teflon-lined autoclave and underwent hydrothermal treatment at 180 ^oC for 24 h. After cooling to room temperature, the white precipitate was collected by centrifugation and washed thoroughly with deionized water twice.

Synthesis of defect-rich MoO_{2-x} cluster anchored nitrogen-doped carbon nanotubes (MoO_{2-x}/NC)

The Mo-dopamine hybrid precursor nanotubes were prepared by a template-mediated co-precipitation method. In a typical procedure, a mixture of MoO_3 nanorods (300 mg), $(NH_4)_6Mo_7O_{24}\cdot 4H_2O$ (300 mg), and dopamine hydrochloride (300 mg) in 8 mL H_2O was blended with 40 mL ethanol. Upon rapid injection of 50 μL $NH_3\cdot H_2O$, a dark red suspension formed readily. The product, collected by centrifugation after 6 h of stirring, was then calcined under H_2/Ar at 600 ^oC for 8 h (5 ^oC min^{-1}) to yield the final MoO_{2-x}/NC composite.

Synthesis of N doped carbon (NC)

The as-obtained MoO_{2-x}/NC composite was subjected to etching by stirring in a mixed solution of concentrated hydrochloric acid (HCl) and nitric acid (HNO_3) at 80 ^oC to remove the MoO_2 clusters. Upon completion of the treatment, the black product was collected, isolated by successive suction filtration and centrifugation, and then dried under vacuum at 60 °C for 12 h to obtain the final NC powder.

Material characterization

The crystallographic structure was determined by Rigaku D/max-ga X-ray diffraction (XRD) equipped with Cu Kα radiation (λ = ~1.54178 Å). The morphology and structure of samples were characterized using a JEOL JSM-IT800 scanning electron microscope (SEM) and a JEM-2100 transmission electron microscope (TEM) with an EDS probe. Thermogravimetric analysis (TGA) was performed on a TAQ 50 thermogravimetric analyzer under an Ar atmosphere up to 600 °C. Thermo Scientific K-alpha X-ray photoelectron spectrometer (XPS) measurements were used to analyzed the surface chemical states, which examined with a monochromatic Al Ka (1486.8 eV) radiation.

Electrochemical measurements

The 2032-type coin cells were assembled in an argon-filled glovebox (H_2O, O_2 < 0.01 ppm). The cathode slurry was prepared by thoroughly mixing the active material, acetylene black, and carboxymethyl cellulose (CMC) in a weight ratio of 7:2:1 in an agate mortar for 30 min. The homogeneous slurry was then coated onto substrates and vacuum-dried at 60 °C for 12 h. The mass loading of electrodes was controlled to be 1.0-2.0 mg cm^{-2}. Sodium metal foil was used as the anode, and 1 M $NaPF_6$ in a mixed solvent of DIGLYME and DOL (1:1 by volume) served as the electrolyte. The specific procedure involves adding 100 μL of electrolyte solution in equal volumes to both sides of the glass fiber separator (GF-D), then assembling the cell with a commercial sodium plate serving as the anode. The cells were initially activated at a low current rate before proceeding to long-term cycling tests. Galvanostatic charge-discharge measurements were carried out using a Neware battery testing system (Shenzhen, China) within a voltage window of 0.5-2.9 V (*vs.* Na^+/Na). Cyclic voltammetry (CV) and electrochemical impedance spectroscopy (EIS) were performed on a CHI660E electrochemical workstation (Shanghai, China).

Calculate the diffusion rate of sodium ion based on CV

By testing the CV curves of different scan rates (0.2, 0.5, 0.8, 1.0, 1.5 mV s^{-1}) within a voltage window of 0.5 V – 2.9 V, the measured peak current can be plotted against the

square root of the scan rate to fit the slope (k) of different samples, which can macroscopically describe the diffusion rate of sodium ion. The calculation process is as follows:

$$i_p = \mathrm{k} \times v^{1/2} \quad (1)$$

According to the Randles Sivick equation:

$$\mathrm{k} = 2.69 \times 10^5 n^{3/2} A D^{1/2} v^{1/2} C \quad (2)$$

Here, i_p represents the peak current, n represents the number of electron transfers in the reaction (for Na^+, n = 1), the A represents the effective area of the electrode (1.13 cm^2), C is the Na^+ concentration in the battery, v represents the scanning rate, and D is the diffusion coefficient of Na^+.

Calculated the diffusion rate of sodium ion based on Galvanostatic intermittent titration technique (GITT)

GITT measurements were taken by charge/discharge at 0.1 C for 30 minutes, followed by 3 h relaxation period until the specified cut-off voltage was reached. The Na^+ diffusion coefficient can be calculated using the following equation:

$$D(Na^+) = 4/(\pi\tau) \times (n_m V_m/A)^2 \times (\Delta E_s/\Delta E_t)^2 \quad (3)$$

Herein, τ, n_m, V_m and A denote the relaxation time, the molar quantity, the molar volume of the electrode material and the surface area of electrode material. In addition, ΔE_s and ΔE_t denote the voltage changes induced by the pulse during constant-current charge/discharge.

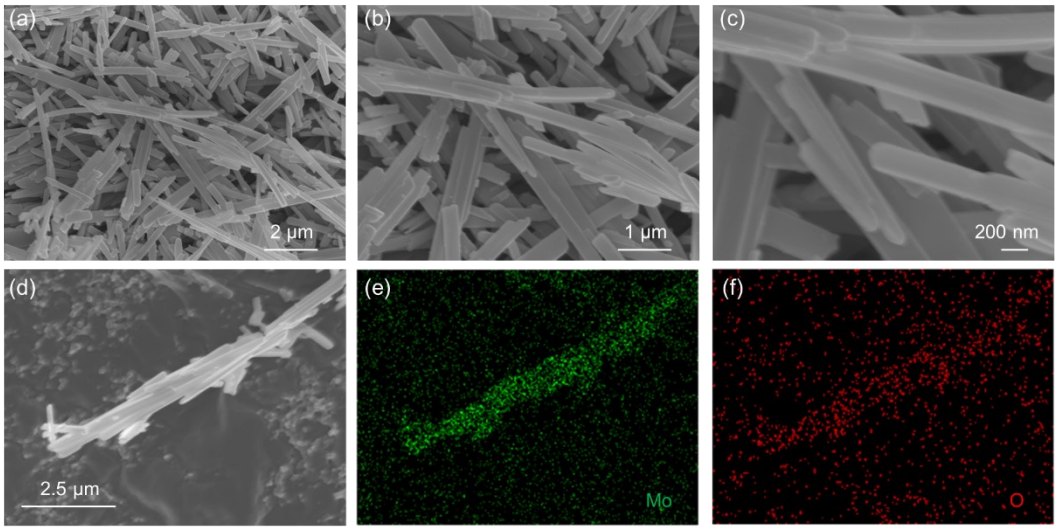

Fig. S1. (a-c) SEM images of the MoO_3 nanorods at different magnifications. (d-f) EDS-mapping image and corresponding elemental mappings of the MoO_3 nanorods.

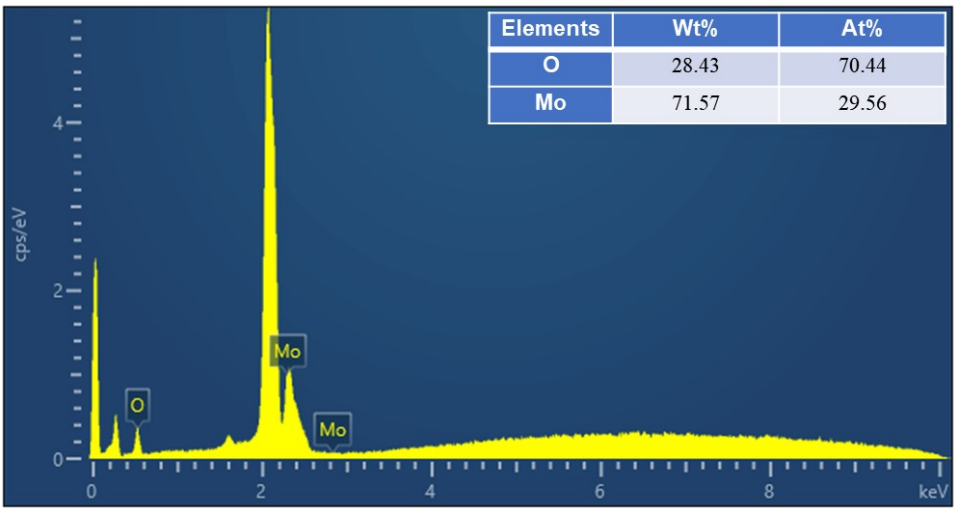

Fig. S2. EDX spectrum of the MoO_3.

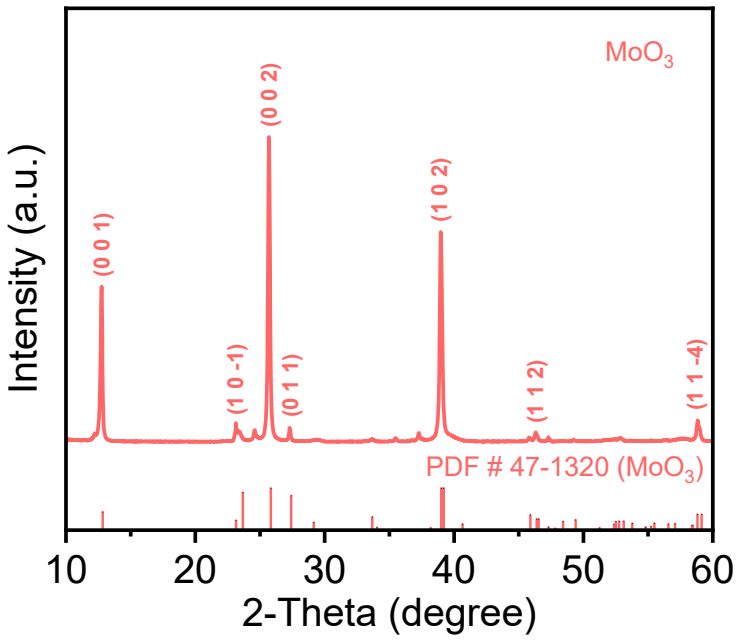

Fig. S3. XRD pattern of the MoO_3 nanorods.

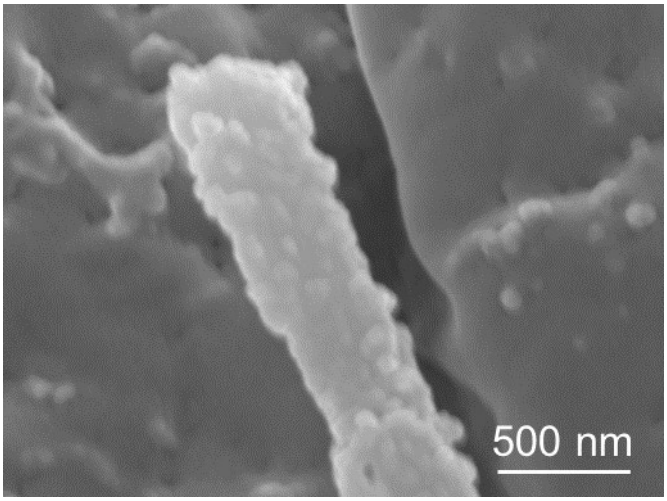

Fig. S4. SEM images of the Mo-dopamine hybrid precursor nanotubes.

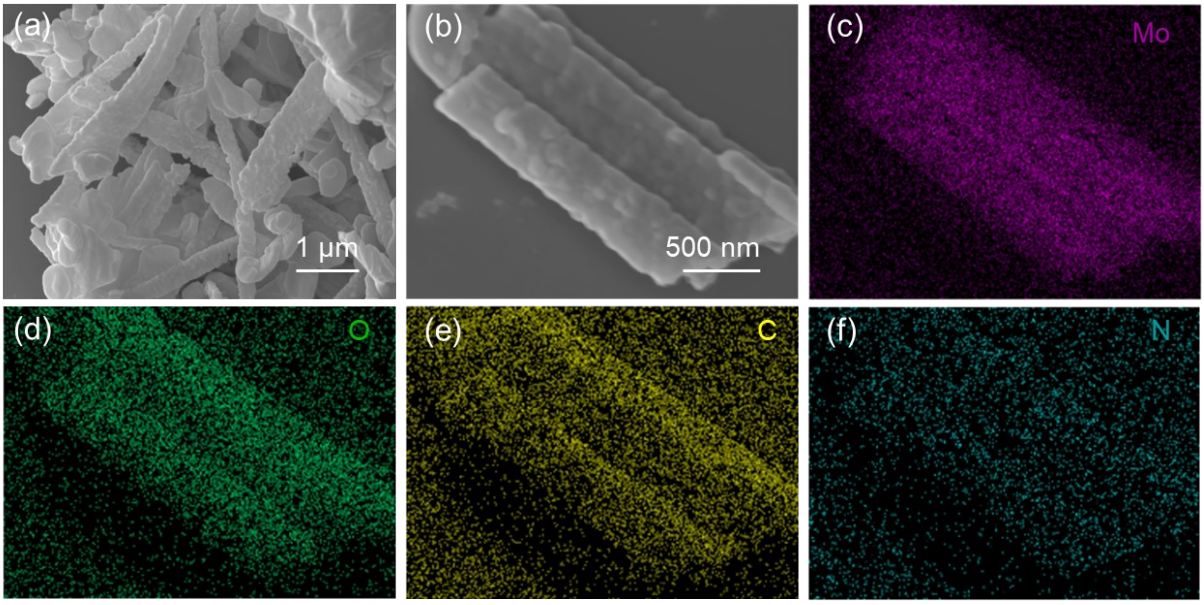

Fig. S5. (a, b) SEM images of the MoO_{2-x}/NC under low magnification and (c-f) EDS mapping at low magnification.

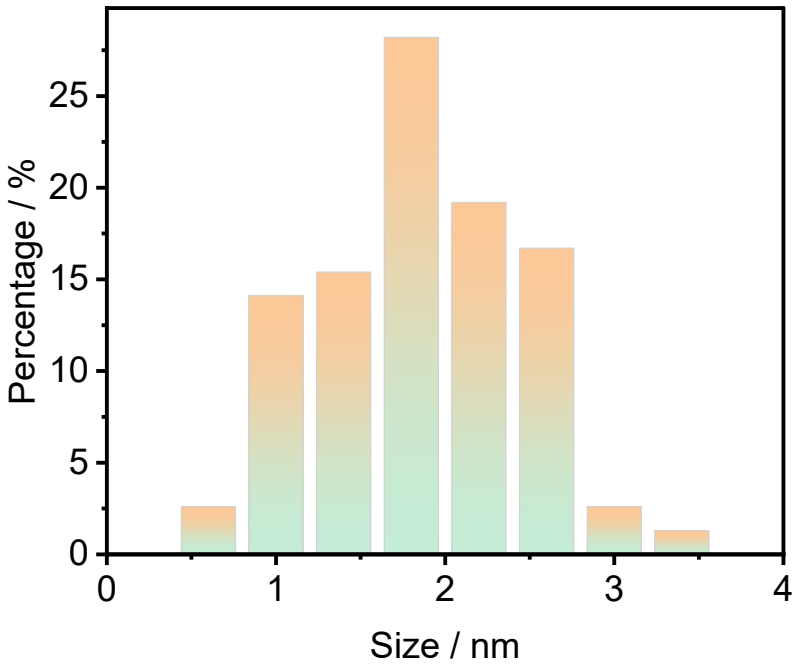

Fig. S6. The size distribution of the MoO_{2-x} clusters on MoO_{2-x}/NC composite materials.

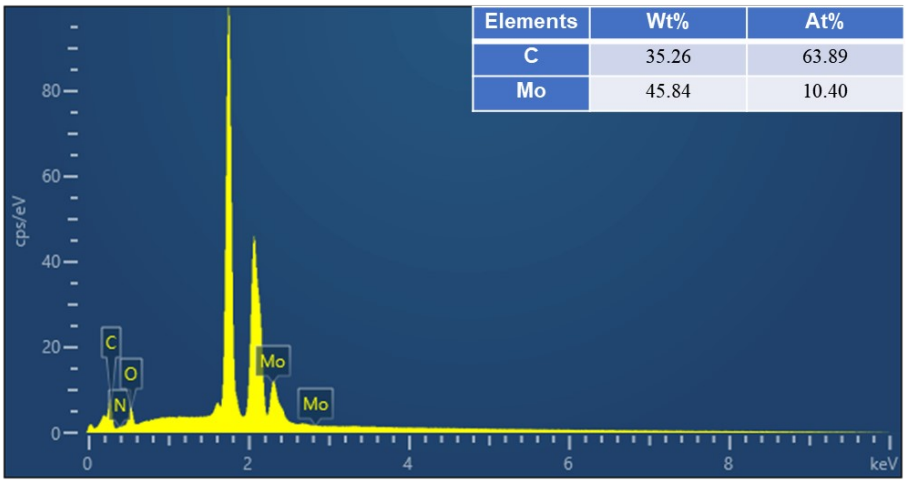

Fig. S7. EDX spectrum of the MoO_{2-x}/NC composite

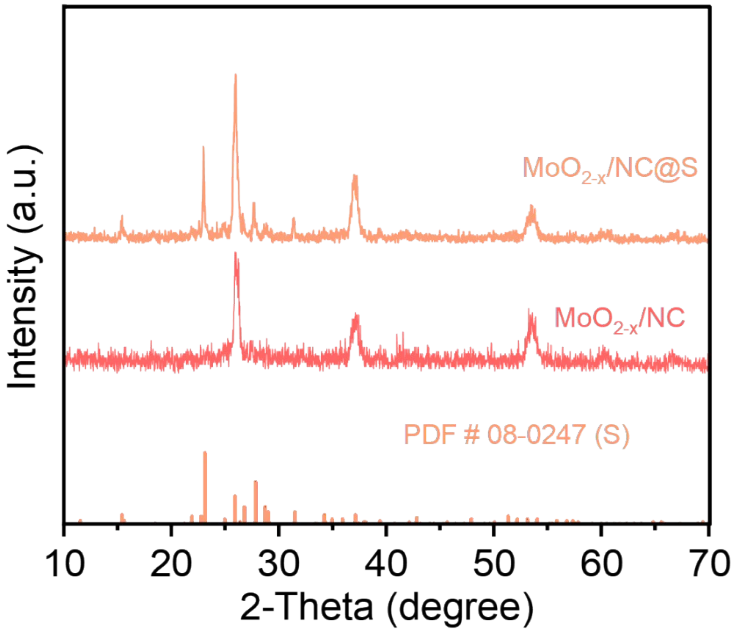

Fig. S8. XRD patterns of MoO_{2-x}/NC and MoO_{2-x}/NC@S.

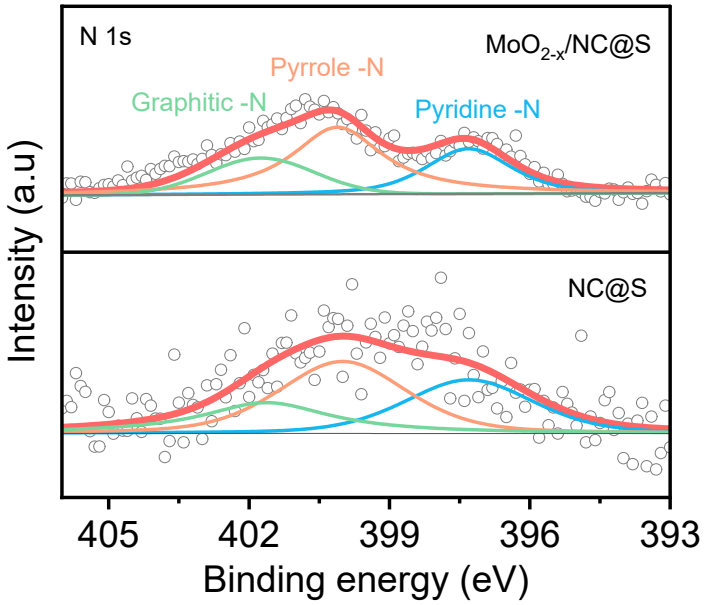

Fig. S9. High-resolution XPS N 1s spectra of the MoO_{2-x}/NC@S.

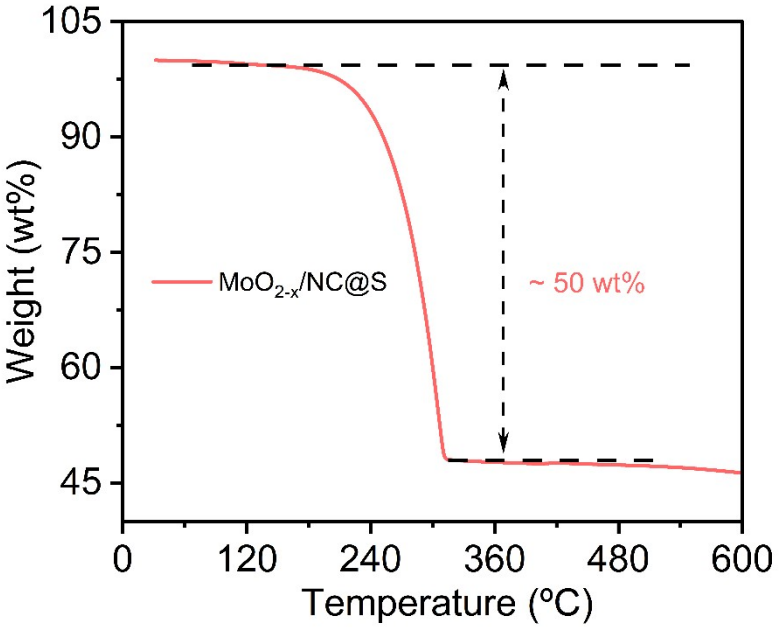

Fig. S10. Thermogravimetric analysis curve of MoO_{2-x}/NC@S.

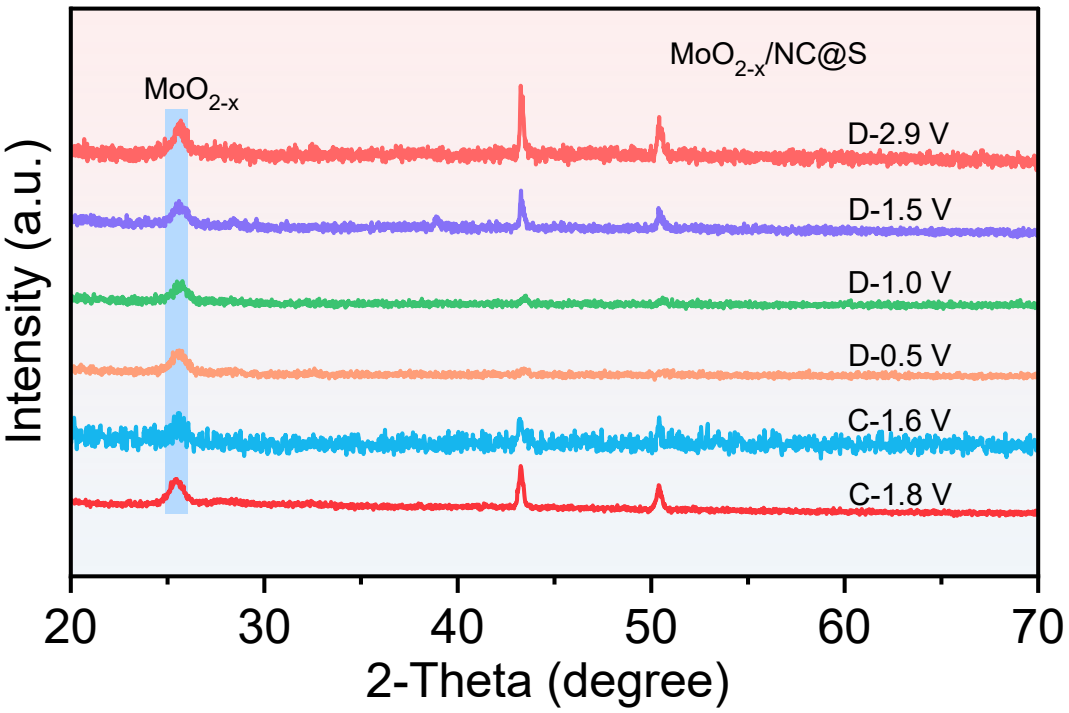

Fig. S11. *Ex-situ* XRD curves of the MoO_{2-x}/NC@S.

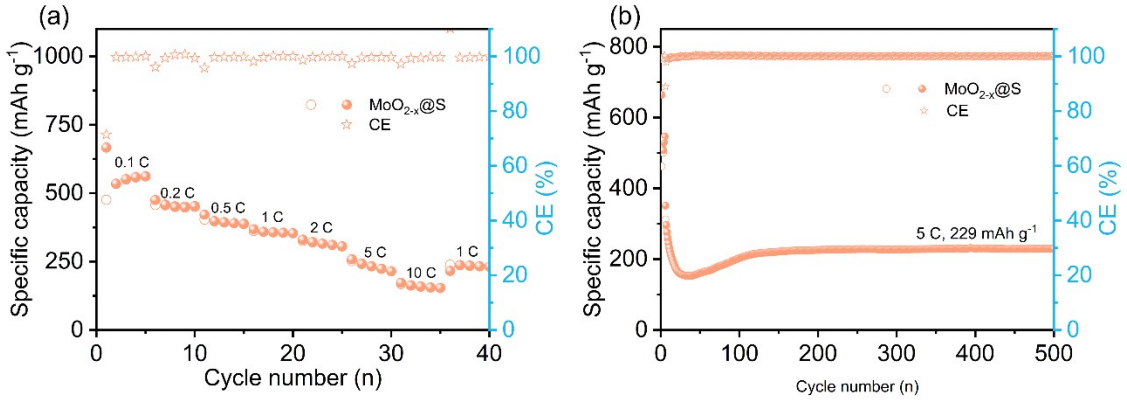

Fig. S12. (a) Rate performance and (b) long-term cycling performance of MoO_{2-x}@S.

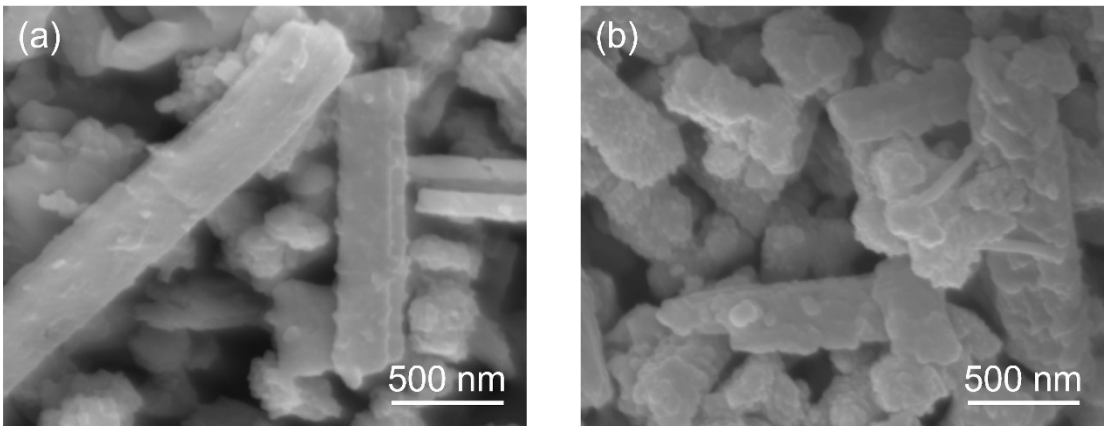

Fig. S13. SEM images of MoO_{2-x}/NC@S (a) initial and (b) after cycling.

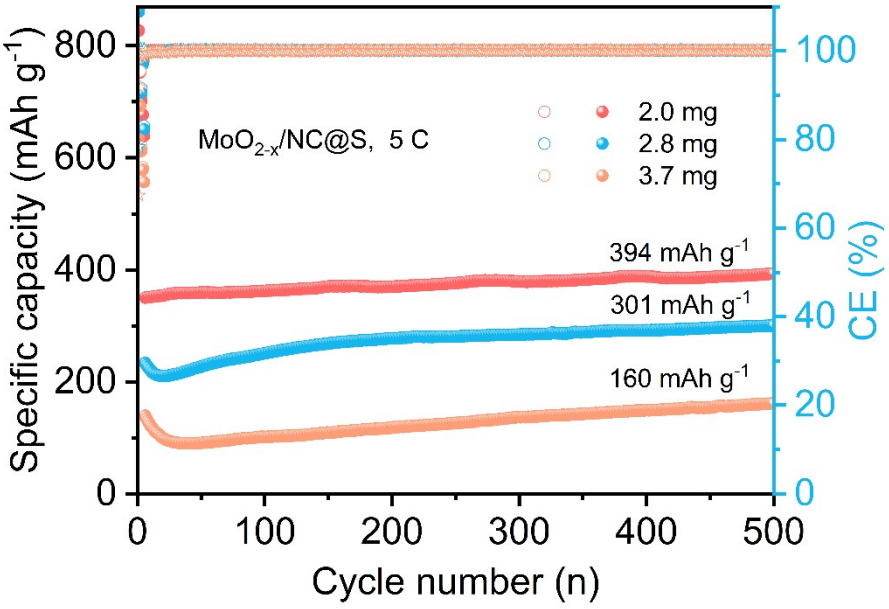

Fig. S14 The performance of MoO_{2-x}/NC@S at different active material loadings.

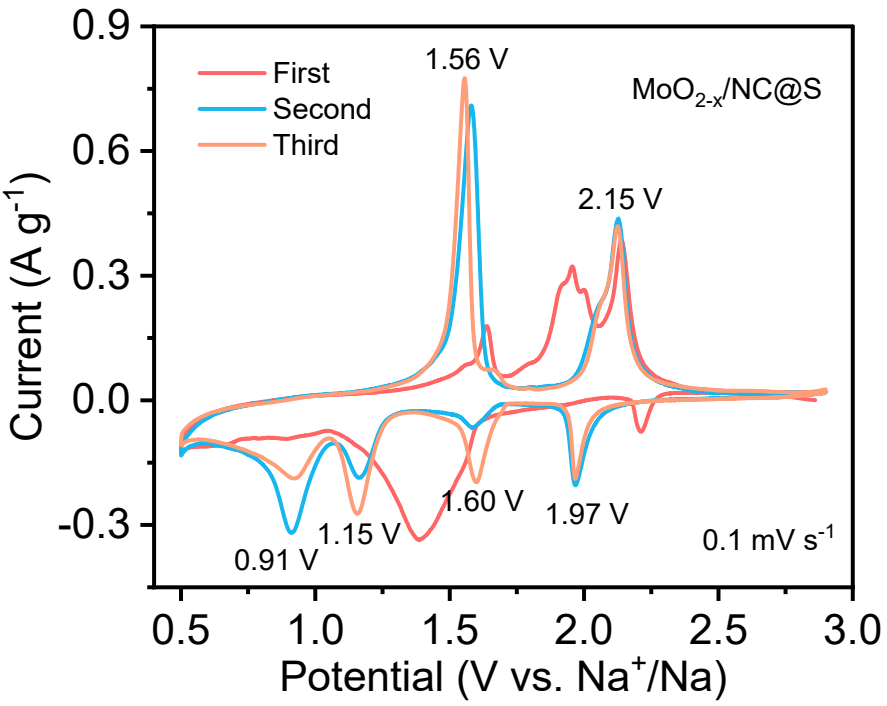

Fig. S15. First three CV curves of MoO_{2-x}/NC@S at a scan rate of 0.1 mV s^{-1}.

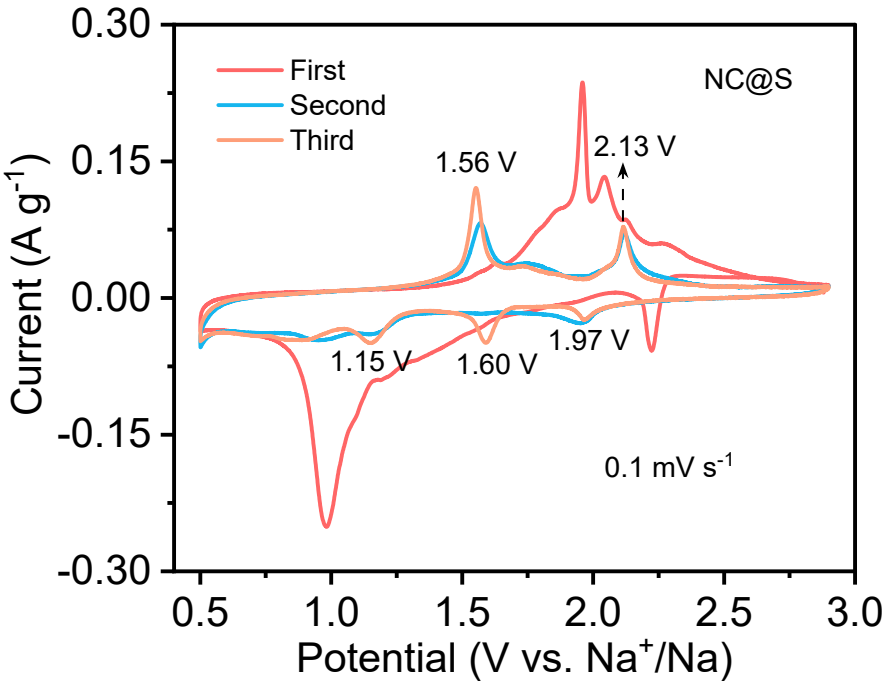

Fig. S16. First three CV curves of NC@S at a scan rate of 0.1 mV s^{-1}.

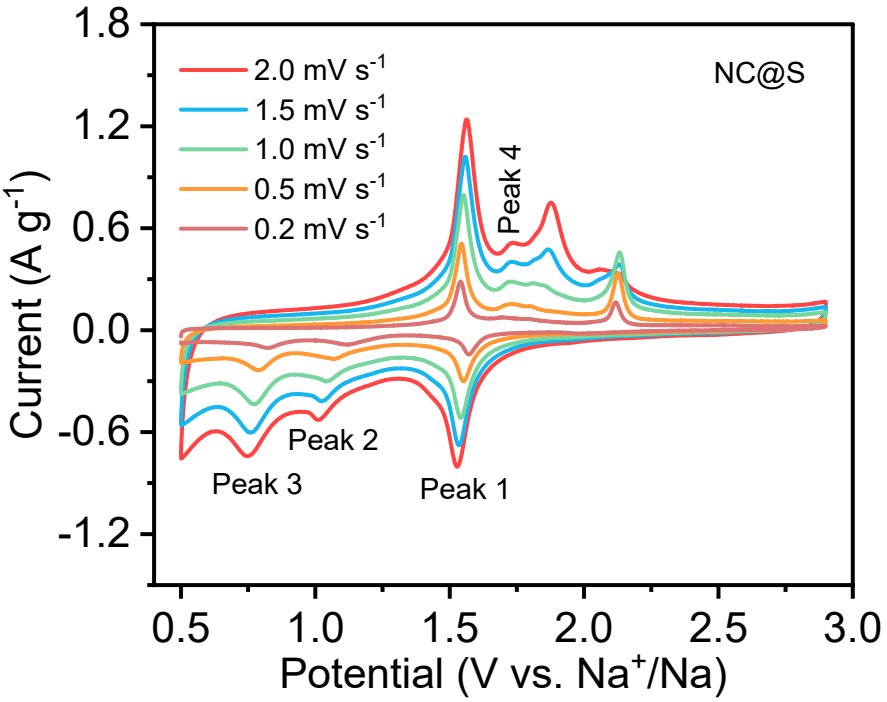

Fig. S17. CV curves of NC@S at various scan rate.

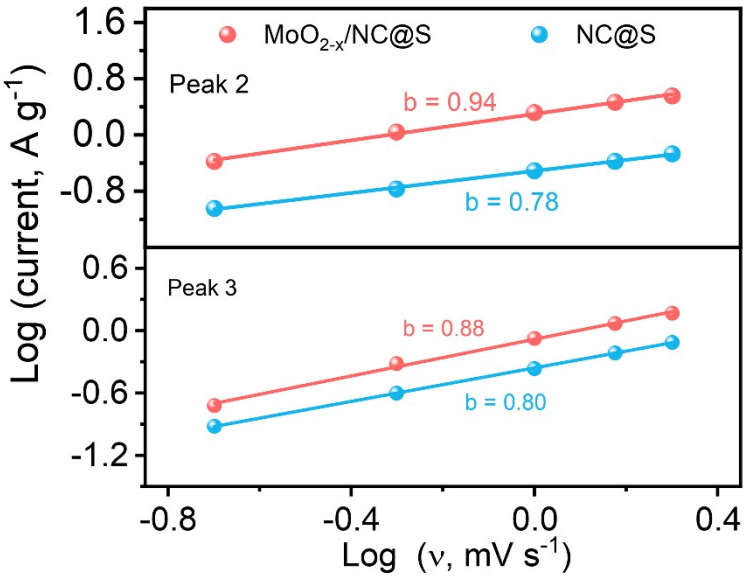

Fig. S18. Slope of the double logarithmic curve based on the scan rate and current density at peak 2.

Table S1. Comparison of the performance of as-prepared MoO_{2-x}/NC@S and other materials in recently reported works

Electrode materials	Initial Capacity/ Current density	Capacity/Cycle number/Current density	Capacity retention rate (%)	References
MoO_{2-x}/NC@S	1069 mAh g^{-1}/ 0.119 A g^{-1}	331 mAh g^{-1}/2000 cycles/8.375 A g^{-1}	94	**This work**
TiO_2@SPC-S	664 mAh g^{-1}/ 0.119 A g^{-1}	283 mAh g^{-1}/400 cycles/2 A g^{-1}	64	*J. Colloid. Interface Sci.* 2025, 684, 235-242
Ni-MoS_2@MPC/S	1432 mAh g^{-1}/ 0.1 A g^{-1}	467 mAh g^{-1}/500 cycles/3A g^{-1}	44	*Chem. Eng. J.* 2025, 514, 163123
S@Mn_1-PNC	989 mAh g^{-1}/ 0.1 A g^{-1}	360 mAh g^{-1}/2000 cycles/2 A g^{-1}	76	*Nat. Commun.* 2024, 15, 3325
S@HPC/Mo_2C	1408 mAh g^{-1}/ 0.2 A g^{-1}	503 mAh g^{-1}/800 cycles/5 A g^{-1}	35	*Adv. Mater*. 2022, 34, 2200479
FeS_2@NCMS/S	1471 mAh g^{-1}/ 0.1 A g^{-1}	395 mAh g^{-1}/850 cycles/1 A g^{-1}	27	*Adv. Mater*. 2020, 32, 1906700
NiS_2@NPCTs/S	760 mAh g^{-1}/ 0.1 A g^{-1}	401 mAh g^{-1}/750 cycles/1 A g^{-1}	42	*Nat. Commun*. 2019, 10, 4793
S@Fe-HC	1023 mAh g^{-1}/ 0.1 A g^{-1}	394 mAh g^{-1}/1000 cycles/0.1 A g^{-1}	39	*Angew. Chem*. 2019, 131,1498
S@Co_n-HC	1081 mAh g^{-1}/ 0.1 A g^{-1}	508 mAh g^{-1}/600 cycles/0.4 A g^{-1}	47	*Nat. Commun.* 2018, 9, 4082
CN/Au/S	830 mAh g^{-1}/ 0.1 A g^{-1}	430 mAh g^{-1}/1000 cycles/2 A g^{-1}	42	*Energy Environ. Sci*., 2020, 13, 562
Core-shell ZCS@S	768 mAh g^{-1}/ 0.5 A g^{-1}	250 mAh g^{-1}/2000 cycles/1 A g^{-1}	26	*ACS Nano* 2020, 14, 6, 7259

Reference

[1] C. Guan, X. Liu, W. Ren, X. Li, C. Cheng, J. Wang, Adv. Energy Mater., 7 (2017) 1602391.
[2] L. Fan, R, Ma, Q. Zhang, X. Jia, B. Lu, Angew. Chem. 2019, 131,10610-10615.
[3] Q. Liu, Z. Hu, Y. Liang, L. Li, C. Zou, H. Jin, S. Wang, H. Lu, Q. Gu, S. Chou, Y. Liu, S. Dou, Angew. Chem. 2020, 132,5197-5202.
[4] W. Li, S. Chou, J. Wang, H. Liu, S. Dou, Nano Lett.2013, 13, 5480-5484.
[5] Y. Huang, Z. Wang, Y. Jiang, S. Li, Z. Li, H. Zhang, F. Wu, M. Xie, L. Li, R. Chen, Nano Energy 2018, 53 524-535.
[6] S. Chen, F. Wu, L. Shen, Y. Huang, S. Sinha, V. Srot, P. Aken, J. Maier, Y. Yu, ACS Nano 2018, 12, 7018-7027.
[7] W. Zhao, X. Ma, G. Wang, X. Long, Y. Li, W. Zhang, P. Zhang, Appl. Surf. Sci. 2018, 445, 167-174.